Engineering Structures 56 (2013) 417–430

Contents lists available at SciVerse ScienceDirect

Engineering Structures

journal homepage: www.elsevier.com/locate/engstruct

Effect of higher modes on the seismic response and design of moment-resisting RC frame structures

Charilaos A. Maniatakis, Ioannis N. Psycharis *, Constantine C. Spyrakos

School of Civil Engineering, National Technical University of Athens, Greece

ARTICLE INFO

Article history:
Received 16 November 2012
Revised 1 May 2013
Accepted 13 May 2013

Keywords:
Higher modes
Frame structures
Modal response
Nonlinear analysis
Reduction factor
Behaviour factor
Design of MRF structures

ABSTRACT

Recently, extensive research has been conducted regarding higher-mode effects on the response of multi degree-of-freedom (MDOF) systems. The research has been focused mainly on structures with a lateral force resisting system consisting of slender walls, since these types of buildings are expected to be mostly affected by higher-mode phenomena according to structural dynamics, and simplified expressions have been proposed for slender-wall structures to account for higher-mode response in estimating shear forces. Current seismic design practice assumes the same reduction factor for all modes, even though there is strong evidence that inelasticity affects higher modes of vibration unequally. Additionally, simplified design methods are based only on the fundamental mode of vibration neglecting the effect of higher modes or considering them as elastic. In this paper, higher-mode contributions on the overall response of a nine-storey moment resisting frame (MRF), for which a domination of the first mode is expected, are investigated. The accuracy of a modified Modal Response Spectrum Analysis (mMRSA) method and other available methods is evaluated by comparing the results with the ones of the nonlinear response history analysis. Modal behaviour (reduction) factors are directly calculated for the first three modes and the validity of common assumptions is examined. The assessment of the methods is not restricted to deformations, but is extended to storey inertial forces and shears as well, which have attracted less interest from structural engineers, even though they are considered responsible for numerous structural and non-structural failures during major recent earthquakes and are critical for the design of several structures, such as precast buildings. The results suggest that the storey inertial forces and accelerations at all storeys and shear forces at higher storeys are significantly underestimated by methods neglecting or non-properly accounting for higher modes, even for first-mode dominated structures. The contribution of higher modes depends on the ground motion characteristics, the overstrength associated with each mode and the response quantity examined.

1. Introduction

The contribution of higher modes to the dynamic response of multi degree-of-freedom (MDOF) systems is an issue of addressed significance affecting the design of new structures and the assessment of existing ones. As a result of higher-mode vibrations, two main phenomena have challenged the interest of engineers during the last decades.

The first phenomenon, known as shear amplification, describes the amplification of shear demands due to higher modes and was firstly addressed by Blakeley et al. [1] for yielding slender walls. The amplification of the shear forces was found to increase with increasing fundamental period and ductility [2,3]. The shear amplification is expected to be more pronounced in slender walls, where the higher modes' effective modal mass is larger and also, well separated periods are observed compared to frames; therefore, it is more likely for slender shear walls to retain the second eigenperiod, T_2, in the acceleration-sensitive region of the response spectrum, affecting the base shear, while the first eigenperiod T_1 is located at the velocity- or even the displacement-sensitive region [4,5]. Several methods can be found in the literature to account for shear amplification [6–8] while an extensive review of the engineering studies regarding shear magnification in RC structural walls can be found in [9].

The second phenomenon, known as floor acceleration magnification, demonstrates the unexpectedly large earthquake-induced accelerations that have been recorded during seismic events or evaluated based on analytical models. During the Northridge, 1994, earthquake, maximum floor accelerations, more than four times the peak ground acceleration, were measured [10]. The floor acceleration magnification phenomenon is strongly related to the inertia forces, since the ratio of the storey inertia force to the storey mass is equal to the storey acceleration in a lumped-parameter

* Corresponding author. Address: Laboratory for Earthquake Engineering, National Technical University of Athens, 9, Heroon Polytechneiou Str., Zografos 15780, Athens, Greece. Tel.: +30 2107721154.

E-mail address: ipsych@central.ntua.gr (I.N. Psycharis).

0141-0296/$ - see front matter © 2013 Elsevier Ltd. All rights reserved.
http://dx.doi.org/10.1016/j.engstruct.2013.05.021

approach of multi-storey structures; thus, an inaccurate evaluation of storey accelerations suggests an imprecise estimation of storey inertial forces. Several indications suggest that numerous failures or even collapse of buildings during past earthquakes were induced by large floor accelerations not expected from the design [11–13]. The accurate calculation of inertial forces is critical for the design of numerous structural components, as diaphragms and connections of precast or steel buildings [14–16], and non-structural components, as equipment [17], which is based on floor accelerations [18–20]. Furthermore, an as-possible-accurate estimation of lateral forces can improve the performance by making more uniform the distribution of maximum inter-storey drifts and enhance design economy [21,22].

Extensive recent research revealed that simplified methods for the calculation of the seismic loads, which are based on the fundamental mode and are adopted by seismic codes, fail to estimate accurately the inertial forces and the seismic floor accelerations [21,23–25]. Recently, Chao et al. [21] showed that significant dispersions can exist between storey inertial forces, which are calculated by the linear static analysis (LSA) (also termed "lateral force method" or "equivalent static analysis") of NEHRP 2003 and International Building Code 2006 provisions and nonlinear response history analysis (NLRHA) results, especially for the upper storeys. This inconsistency was also observed during pseudo-dynamic tests that were conducted with precast concrete buildings [26,27]. It was shown that the storey forces do not follow a decreasing tendency from the upper to the lower levels, as it would be expected by a first mode dominated response, even in the case of a fully regular and symmetric three-storey precast building [27].

In order to determine the maximum seismic demand for the design of new structures, modern seismic codes, including Eurocode 8 (EC8) [28] adopt multi-modal analysis procedures, such as the standard Modal Response Spectrum Analysis (MRSA) (also termed "linear dynamic" analysis) where the maximum base shear is given as a combination of the maximum modal responses. This method, even though it is widely accepted and used by contemporary codes and is well established in engineering practice, has, among others, two significant shortcomings in view of the previous discussion:

(1) A single value for the yield reduction factor R_y (also called behaviour factor, q_y) is considered for all significant modes of vibration.
(2) Design spectral values are calculated using the elastic periods without accounting for the critical change of stiffness during the development of inelasticity.

However, recent studies have shown that the ductility demand associated with higher modes might be significantly reduced [29,30]. For buildings with main lateral force resisting system comprised of structural walls, it was shown that the modal reduction factors decrease with increasing order of modes [23] and that the assumption of elastic behaviour for higher modes may lead to reasonable results [30]. However, limited available results on frame structures have shown that inelasticity can also affect higher modes. Applying a Multi-Mode Pushover procedure (MMP), Sasaki et al. [31] provided evidence that there is a possibility that the 2nd mode exceeds the elastic limit, while the 1st and 3rd modes remain elastic. In other words, it is possible that a higher mode turns nonlinear while lower modes remain linear, as was shown by Paret et al. [32] for a 17-storey steel frame building. Thus, the assumption that the reduction factors R_y decrease with increasing mode-order might be inaccurate in several cases. It is noted that, although local ductility is evidently related to the total deformation of the structure, under the assumption that modal analysis can be extended to nonlinear response member deformations are associated with the corresponding modal displacements and, thus, the notion of modal ductility can be established. On the other hand, the assumption of elastic higher-mode response might result in conservative predictions of storey shear forces [33]. Indicating the inconsistency of using the elastic modes for inelastic behaviour, Sullivan et al. [34] proposed a new modal superposition method that uses transitory inelastic modes.

Except of the standard MRSA method, several nonlinear static procedures (NSP) (or push-over analyses) have been proposed to evaluate the seismic performance of MDOF structures. EC8 [28] incorporates the N2 method, originally proposed by Fajfar and Fischinger [35]. However, the selection of a single lateral force distribution is believed to provide accurate results only for structures dominated by the first mode. To assess the contribution of higher modes of MDOF structures, several multi-mode pushover methods have been proposed in the literature [36–40]. Some of them imply an adaptive lateral load vector [41,42], while others attempt to capture the probabilistic nature of the seismic response and the continuous modification of the dynamic characteristics of MDOF systems at different intensity levels [43]. A detailed discussion on some of these methods can be found in [42]. Finally, several seismic codes and design standards, such as Eurocode 8 [28], ASCE/SEI 7-05 [44] and Tall Buildings Initiative [45], suggest, as an alternative to the common MRSA, LSA or NSPs methods, to conduct a number of NLRHA in order to properly account for higher mode effects. The proper selection and scaling of the seismic records to be used as base excitations remains an issue of research [46].

In the investigation presented herein, higher mode effects on a nine-storey RC plane frame structure are examined. The selected frame meets the provisions of Eurocode 8 [28] for the assessment of the inelastic response through a single-mode pushover procedure. For the estimation of higher-mode effects, the Uncoupled Modal Response History Analysis (UMRHA) method is applied. The method was originally developed as a precursor of the MPA method [36]. A modified Modal Response Spectrum Analysis (mMRSA) is also proposed, which, in contrast to the standard MRSA, uses inelastic response spectra without assuming a unique value of R_y for all modes. The idea of using inelastic spectra or empirical R_y–μ formulas for the calculation of the maximum modal displacements and accelerations was also proposed by Goel and Chopra [47] as a possible simplification of MPA. However, in mMRSA, storey deformations and internal forces are not extracted from the pushover database as in MPA, but are directly calculated from the modal responses as explained in the following section.

The effectiveness of these methods and other commonly used ones, as the standard MPA [36], the modified MPA [37], the N2 [35] and the extended-N2 [39], is assessed by comparison of the results for a set of earthquake records with the ones of NLRHA. It must be noted that there are other methods available in the literature which may also provide results of the same accuracy, as for example the Modified Modal Superposition method (MMS) proposed by Priestley and Amaris [29] and other similar ones that consider elastic response for higher modes. Those methods, however, are more oriented at design, while this study is more centered on evaluating the ductile response of higher modes.

The results of the analyses show that the inertial forces may be strongly affected by the higher modes of vibration even for a first-mode dominated frame structure. The suggested mMRSA procedure, and the other examined multimode pushover methods such as MPA, may provide an accurate estimation of these forces, while N2 leads to non-conservative results.

2. Considered methods of analysis

The results that are presented in the next section were obtained using several methods for the nonlinear analysis of structures that are briefly presented in the following. Most of them are based on the combination of modal responses. It should be noted, however, that the application of modal analysis to nonlinear response, which has been widely adopted in the design of new structures and the assessment of the capacity of existing ones, is an assumption that lacks conceptual accuracy, because: (i) the spread of inelasticity in structural members produces a continuous reduction in stiffness that changes mode shapes; and (ii) the coupling between modes can be neglected for low levels of inelasticity only. Even though the modification of mode shapes is directly or indirectly addressed by many methods, the application of modal analysis to study damage that implies high levels of nonlinearity, based on an assumption valid for minor excursions into the nonlinear range, remains a shortcoming of these methodologies.

2.1. NLRHA method

In case of inelastic behaviour, the differential equation that governs the response of an MDOF structure with N degrees of freedom is [6]:

$$[m]\cdot\{\ddot{u}\}+[c]\cdot\{\dot{u}\}+\{f_S\}(\{u\},sign\{\dot{u}\})=-[m]\cdot\{i\}\cdot\ddot{u}_g(t) \quad (1)$$

where $[m]$ and $[c]$ are the mass and damping matrices of the system; $\{u\}$ is the lateral displacements vector; $\{i\}$ is the influence vector; $\{f_S\}$ is the vector of nonlinear lateral forces which depend on the history of the deformation; and $\ddot{u}_g(t)$ is the ground acceleration.

In the standard Non-Linear Response History Analysis (NLRHA), which is generally considered the most accurate among the available methods of nonlinear analysis, Eq. (1) is solved numerically. In the original presentation of most of the procedures mentioned in the Introduction, the results were compared with the NLRHA considering this method as the reference method to assess accuracy. However, it should be kept in mind that the accuracy of NLRHA might be sensitive to the integration technique applied. Dokainish and Subbaraj [48] and Subbaraj and Dokainish [49] provided a comprehensive discussion on relative merits, computational aspects and stability issues of some of the most popular available direct time-integration methods. For the analyses presented herein, SAP 2000 [51] was employed to determine the nonlinear response, which uses the Hilber-Hughes-Taylor alpha method to solve Eq. (1). It should be noted, however, that more elaborate integration schemes than NLRHA are available today, such as time stepping approaches with prescribed functions for displacement and acceleration within each time step [50].

2.2. UMRHA method

The Uncoupled Modal Response History Analysis (UMRHA) method is a valuable tool to account for higher mode effects, since it allows examining time-history response for each separate mode of vibration taking into consideration inelasticity [36].

Chopra and Goel [36] showed that the coupling between normal modes can be neglected in relatively low levels of inelasticity and, thus, the superposition rule can be expanded to inelastic behaviour. Based on this assumption, instead of Eq. (1), N independent nonlinear equivalent SDOF systems may be solved, governed by the following equation of motion, valid for the nth degree of freedom:

$$\ddot{D}_n(t)+2\cdot\zeta_n\cdot\omega_n\cdot\dot{D}_n(t)+\frac{F_{sn}}{L_n}=-\ddot{u}_g(t) \quad (2)$$

where $D_n(t)$ is the time history of the deformation and dot denotes differentiation with respect to time; ζ_n and ω_n are the damping ratio and natural frequency of the nth mode, respectively; F_{sn} is the lateral resisting force for the nth mode and L_n is the nominator of the participation factor Γ_n given by

$$\Gamma_n=\frac{L_n}{M_n},\quad L_n=\sum_{n=1}^{N}m_j\cdot\varphi_{jn},\quad M_n=\sum_{n=1}^{N}m_j\cdot(\varphi_{jn})^2 \quad (3)$$

In Eq. (3), m_j is the mass associated with the jth degree of freedom and φ_{jn} is the jth component of the nth mode. The lateral force–displacement relationships, F_{sn}/L_n–D_n, for the equivalent SDOF system can be obtained in two steps, as shown in Fig. 1: firstly pushover analyses are performed for the MDOF system for constant shaped lateral force vectors$\{s_n^*\}=[m]\cdot\{\varphi_n\}$ and the base shear versus roof displacement curves, V_{bn}–u_{rn}, are obtained; and secondly the V_{bn}–u_{rn} curves are transformed to F_{sn}/L_n–D_n applying the following equations:

$$\frac{F_{sny}}{L_n}=\frac{V_{bny}}{L_n\cdot\Gamma_n}\quad D_{ny}=\frac{u_{rny}}{\Gamma_n\cdot\varphi_{rn}} \quad (4)$$

where the subscript 'y' denotes yielding and the subscript 'r' denotes roof. Note that $F_{sny}/L_n = A_{ny}$, the yield acceleration. The numerical solution of Eq. (2) allows estimating the contribution of the nth mode to the overall response by applying the following equation, similarly to the elastic behaviour:

$$\{u_n(t)\}=\{\varphi_n\}\cdot\Gamma_n\cdot D_n(t) \quad (5)$$

while the total response is obtained from the superposition of the modal contributions.

2.3. MPA and MMPA methods

The MPA method is a simplification of the UMRHA method according to which the peak deformation D_n of the nth SDOF system is calculated by a pushover analysis instead of solving Eq. (2). The corresponding maximum roof displacement, u_{rn}, of the MDOF system is determined applying Eq. (5). The desired response values for each mode are extracted from the pushover databases for the corresponding maximum roof displacement and the modal responses are combined applying typical combination rules as SRSS and CQC.

A modified version of MPA (denoted MMPA) has been proposed by Chopra et al. [37], according to which a single pushover is performed for the first mode only and the contribution of the higher modes is calculated for elastic response. The consideration of elastic response for higher modes has been widely adopted in the literature, e.g. [3,8,29].

2.4. mMRSA method

The method mMRSA is proposed here as a modification of MPA that uses the concept of the standard Modal Response Spectrum Analysis (MRSA). The method considers modal uncoupling similarly to MPA and UMRHA. In contrast to the standard MRSA, in which the higher modes are considered with the same reduction factor as the first mode, in mMRSA different reduction factors, R_y are applied to each mode. The assumption of a single R_y for all modes is not valid and leads to an underestimation of floor shear forces and accelerations. In mMRSA, the actual reduction factor, R_{ny}, is calculated for each mode n from the equation:

$$R_{ny}=\frac{SA_{el}(T_n,\zeta_n)}{A_{ny}} \quad (6)$$

where SA_{el} is the elastic spectral acceleration. As observed by Sasaki et al. [31] and will be shown in the ensuing, the resulting reduction factors are neither the same for all modes, nor are equal or less than one for all higher modes denoting elastic behaviour. Their value depends on the structure characteristics and the shape of the response spectrum.

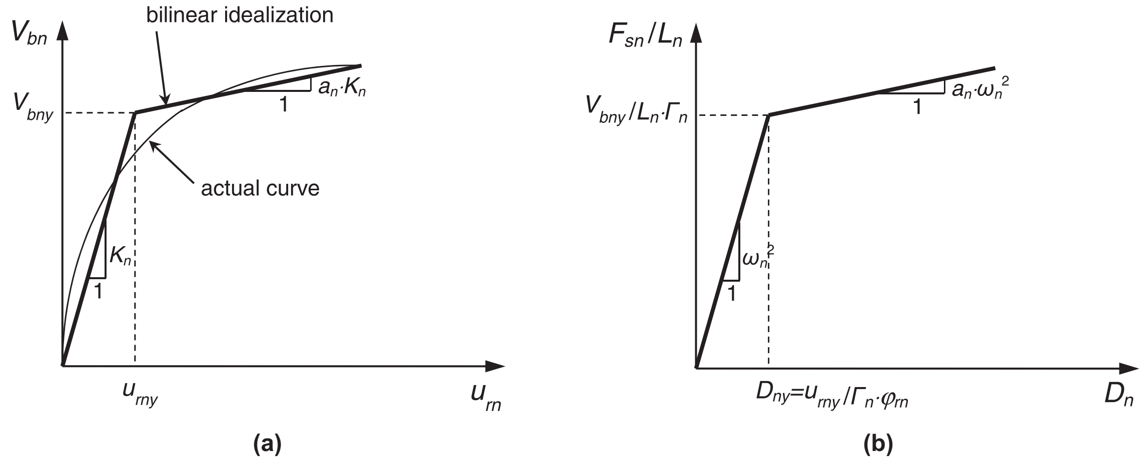

Fig. 1. (a) V_{bn}–u_{rn} pushover curve of the nth mode; (b) corresponding F_{sn}/L_n–D_n relationship for the equivalent SDOF inelastic system.

In case that the post-yield stiffness of the equivalent SDOF system is zero, the maximum inelastic acceleration, A_n, is equal to the yield acceleration, A_{ny}. For systems with positive post-yield stiffness, A_n will be larger than A_{ny}. Both the maximum acceleration A_n and the maximum displacement D_n can be calculated either from inelastic spectra or by applying proper relationships (R_y–μ relationships) available in the literature (e.g. [52]). The plasticity index μ_n of the nth mode is equal to the ratio of the maximum displacement D_n over the yield displacement D_{ny} of the equivalent SDOF system:

$$\mu_n = \frac{D_n}{D_{ny}} \tag{7}$$

With A_n and D_n known for each equivalent SDOF, the modal maxima for the MDOF system can be calculated and the total response can be determined applying a standard combination rule, as SRSS or CQC similarly to the standard MRSA.

The steps of the mMRSA method can be outlined as follows:

Step 1: Estimate the dynamic characteristics of the elastic MDOF system, specifically natural frequencies ω_n and mode vectors $\{\varphi_n\}$.
Step 2: Perform pushover analyses for the first K modes that are considered significant for the overall response with constant lateral force vectors $\{s_n^*\} = [m] \cdot \{\varphi_n\}$ and produce V_{bn}–u_{rn} curves.
Step 3: Convert the pushover curves to bilinear form [36] and determine V_{bny} and u_{rny}.
Step 4: Develop the F_{sn}/L_n–D_n relationships using Eq. (4).
Step 5: Calculate the maximum displacement D_n and maximum acceleration A_n of the equivalent nth inelastic SDOF as described above.
Step 6: Calculate the maximum response quantities for the nth mode at the jth level from the following equations:

$$\left.\begin{aligned} u_{jn} &= \Gamma_n \cdot \varphi_{jn} \cdot D_n \\ F_{jn} &= \varphi_{jn} \cdot \Gamma_n \cdot m_j \cdot A_n \\ IDR_{jn} &= \tfrac{\varphi_{jn}-\varphi_{j-1,n}}{h_j} \cdot \Gamma_n \cdot D_n \\ V_{jn} &= \sum_{l=j}^{N} \Gamma_n \cdot m_l \cdot \varphi_{ln} \cdot A_n \end{aligned}\right\} \tag{8}$$

where u, F, IDR and V denote displacement, storey inertial force, inter-storey drift and storey shear force, respectively.

Step 7: Evaluate the total response quantities applying a standard combination rule, e.g. SRSS, to combine the modal quantities of the K important modes:

$$\left.\begin{aligned} u_j &= \sqrt{\textstyle\sum_{n=1}^{K} u_{jn}^2} = \sqrt{\textstyle\sum_{n=1}^{K} (\Gamma_n \cdot \varphi_{jn} \cdot D_n)^2} \\ F_j &= \sqrt{\textstyle\sum_{n=1}^{K} F_{jn}^2} = \sqrt{\textstyle\sum_{n=1}^{K} (\varphi_{jn} \cdot \Gamma_n \cdot m_j \cdot A_n)^2} \\ IDR_j &= \sqrt{\textstyle\sum_{n=1}^{K} IDR_{jn}^2} = \sqrt{\textstyle\sum_{n=1}^{K} \left(\frac{\varphi_{jn}-\varphi_{j-1,n}}{h_j} \cdot \Gamma_n \cdot D_n\right)^2} \\ V_j &= \sqrt{\textstyle\sum_{n=1}^{K} V_{jn}^2} = \sqrt{\textstyle\sum_{n=1}^{K} (\sum_{l=j}^{N} \Gamma_n \cdot m_l \cdot \varphi_{ln} \cdot A_n)^2} \end{aligned}\right\} \tag{9}$$

The mMRSA method described above is similar to MPA and resembles the standard, design oriented, Modal Response Spectrum Analysis (MRSA). The pushover analyses performed within Step 2 are only used to determine the characteristics of the equivalent SDOF systems, while the other maximum response quantities r_n are not extracted from the pushover databases as in MPA but can be evaluated based on the deformations and forces of each mode according to Eq. (8). For example, the rotations can be evaluated based on maximum IDR values. Similarly, the estimation of storey forces for the nth mode can be obtained from the maximum acceleration A_n instead of calculating them from the column shears corresponding to the maximum roof displacement, which would be extracted from the pushover database and added according to the standard MPA. In this sense, mMRSA can be thought as a simplification of the MPA method [47].

The mMRSA method retains some of the significant shortcomings of the NSPs and MPA methods, specifically:

(i) Further research is needed to assess the error introduced by omitting the coupling of modes during inelastic response.
(ii) The development of V_{bn}–u_{rn} pushover curve for each mode is not always possible due to changes in the direction of the roof deformation with increasing lateral load, a phenomenon termed as "reversal" [53]. The reversals might be related to the formation of a local plastic mechanism, not detected by the traditional 1st mode NSPs. Thus, when a new structure is designed, a reversal associated with a higher mode might require modifications in strength or ductility to avoid this possible mechanism.
(iii) The method might not be accurate for stiffness-degrading systems [54].
(iv) Proper modifications should be made for plan-asymmetric structures where the translational and torsional motions are coupled.

2.5. Standard and extended N2 methods

The method N2 [35] is similar to MPA, but only the first mode is considered. The equivalent linear SDOF system is considered elastic–perfectly plastic without post-yield stiffness. The response is calculated using R_y–μ relations. An improvement of this method was proposed by Kreslin and Fajfar [39] (extended N2), in which higher modes are also considered but assuming that they respond elastically. The final response of a MDOF structure is calculated from a combination of the standard N2 method and an elastic MRSA. In the extended N2 method [39], the final response of a MDOF structure is calculated by the results of the standard N2 method applying a correction factor that considers higher modes through a scaled elastic MRSA. It is suggested that for local quantities the correction factors obtained from storey drifts should be applied.

3. Case study

The above-mentioned methods were applied in a case study for the evaluation of their accuracy, using the results of NLRHA as the basis of comparison, and the assessment of higher mode effects. For this case study, the central frame of a nine storey plan-symmetric reinforced concrete building was selected. The building was designed according to the Greek seismic design code EAK 2000 [55] for ground acceleration 0.24 g and behaviour (reduction) factor q = 3.5. The floor plan of the building and the elevation of the frame are shown in Fig. 2. The analyses were performed using SAP 2000 [51]. Beams and columns where modelled as linear elements with tri-linear plastic hinges at their ends.

The dynamic characteristics of the equivalent inelastic SDOF systems for the first three modes are given in Table 1. Note that the modal mass participating ratios for the 1st, 2nd and 3rd modes are approximately 80%, 10% and 4%, respectively. Therefore, the structure might be considered as first-mode dominated according to the modal mass criterion employed by seismic codes, which require that a total effective modal mass of at least 90% of the total structural mass should be accomplished for an acceptably accurate MRSA analysis [28]. This provision is based on the fact that the effective modal mass is critical for the contribution of each mode to the base shear. It should be noted, however, that the actual contribution of the nth mode to the response of the structure is also related to the spectral ordinate A_n corresponding to the natural period T_n and damping ratio ζ_n [5], thus it might be significantly different for different quantities. For example, for structures with long first period, the spectral acceleration of the first mode is generally much smaller than the one of the second mode, thus, the contribution of the second mode to the inertial forces might be significant. Concerning displacements, however, the spectral amplitudes generally increase with period; therefore the contribution of the first mode is expected to be indeed dominant. The accuracy of assuming a domination of the first mode for the nonlinear response of the considered frame will be assessed in the ensuing.

Table 1
Dynamic properties of the equivalent inelastic SDOF systems for the three first modes of vibration.

Property	Mode 1	Mode 2	Mode 3
L_n (kN s^2/cm)	6.25	2.18	1.41
Γ_n	1.297	0.463	0.294
F_{sny}/L_n (cm/s^2)	68.41	594.41	1619.14
D_{ny} (cm)	4.9	6.5	6.4
T_n (s)	1.681	0.658	0.396

The frame is regular in elevation and has a fundamental period T_1 = 1.68 s, which is smaller than 2.0 s and four times larger than the transition period T_C between the constant spectral acceleration and the constant spectral velocity regions of the design spectrum. Therefore, according to Eurocode 8 – part 1 [28], the contribution of the higher modes can be neglected in the design and the Lateral Force Analysis (LFA) method can be applied. Also, N2 method can be applied according to Eurocode 8 – part 3 [56].

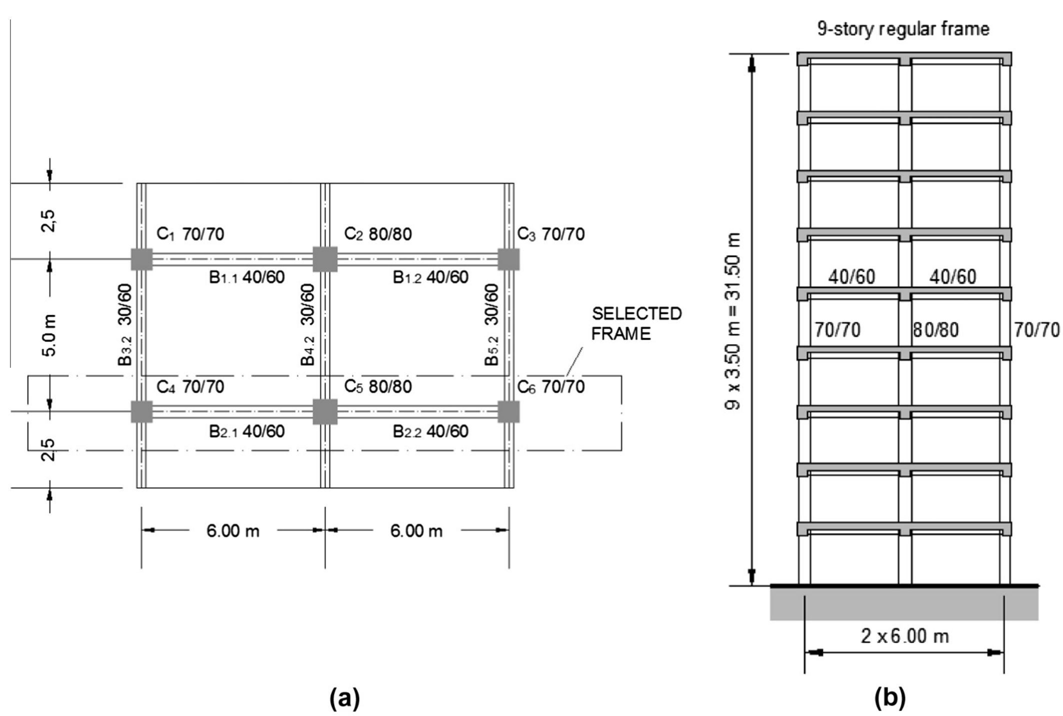

Fig. 2. Case study structure selected for the analysis: (a) typical floor plan of the building and (b) elevation view of the 9-storey central frame.

Nonlinear response history analyses were performed for 34 earthquake records selected from the NGA database [57] and including some major Greek earthquakes [58]. The selected records have different duration, frequency and energy characteristics. Table 2 summarizes the main characteristics of the selected earthquake ground motions, while in Fig. 3 the elastic response spectra of all records and their average spectrum are compared with the design spectrum. It is seen that the selected earthquakes correspond to significantly stronger ground motions than the design earthquake, which was done in purpose in order to produce inelastic response not only of the first mode but also of the second or even the third mode if possible. It is noted that, although the spectral acceleration values of the second and third modes are high for most records, inelastic response of these modes was not certain, since the corresponding yield accelerations of the equivalent SDOFs are also large (Table 1).

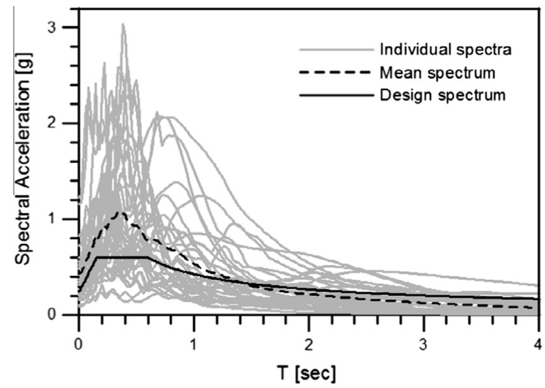

Fig. 3. Comparison of the mean acceleration spectrum of the seismic records selected and the design spectrum for 5% damping.

4. Presentation of the results

4.1. Contribution of higher modes to the response

In order to study the higher mode effects on the response of the RC planar frame described above, nonlinear analysis using UMRHA were performed for the 34 base excitations shown in Table 2. This method has the advantage that allows studying the time histories of modal displacements and accelerations, similarly to the NLRHA. The first three modes of vibration were considered in these analyses. In the results presented herein, member forces, as bending moments of the structural members, are not included, since emphasis is given on the two most important higher-mode phenomena, namely the shear amplification and the floor acceleration magnification, which involve global forces. It is noted, however, that in multi-mode nonlinear procedures, member forces must be calculated from member deformations, using the member force–deformation relationship, and not from the superposition of the modal contribution, since the latter may lead to member forces that exceed the specified member capacity [54].

As a representative case, the results of UMRHA for the ELC180 component of the Imperial Valley (1940) record are presented in detail. Time histories of the obtained results at storey levels 1, 5 and 9 are shown in Fig. 4, while snapshots at the time of maximum top displacement and the time of maximum base shear are given in Fig. 5. From Figs. 4a and 5a it can be observed that the 2nd and the 3rd mode contribution to the storey displacements is very small. A simple explanation can be given by studying the elastic response spectra of the record shown in Fig. 6. Note that for the specific

Table 2
Characteristics of earthquake records used in the study.

Event	Year	Station	M_W	Record	$R_{epicentral}$ (km)	PGA (cm/s^2)	PGV (cm/s)
Imperial Valley, USA	1940	117 El Centro Array #9	7.0	ELC180	13.0	307.1	29.8
				ELC270	13.0	210.9	30.2
Kern Country, USA	1952	USGS 1095 Taft Lincoln School	7.4	TAF021	43.5	153.0	15.3
				TAF111	43.5	174.6	17.5
San Fernando, USA	1971	CDMG 279 Pacoima Dam	6.6	PCD164	11.9	1202.7	112.5
				PCD254	11.9	1138.0	54.3
Friuli, Italy	1976	8023 Buia	5.9	BUI000	17.1	107.9	10.2
				BUI270	17.1	89.3	10.6
Friuli, Italy	1976	8012 Tolmezzo	6.5	TMZ000	20.2	344.3	22.0
				TMZ270	20.2	309.0	30.8
Imperial Valley, USA	1979	USGS 5053 Calexico Fire Station	6.5	CXO225	17.7	269.8	21.2
				CXO315	17.7	198.2	16.0
		5055 Holtville Post Office		HVP225	19.8	248.2	48.8
				HVP315	19.8	216.8	49.8
		USGS 952 El Centro Array #5		E05140	27.8	509.1	46.9
				E05230	27.8	371.8	90.5
Kalamata, Greece	1986	Kalamata 1	6.0	KAL-L	12.0	229.3	30.9
				KAL-T	12.0	263.9	24.0
Loma Prieta, USA	1989	47381 Gilroy Array #3	6.9	G03000	31.4	544.5	35.7
				G03090	31.4	360.0	44.7
Erzincan, Turkey	1992	95 Erzincan	6.7	ERZ-NS	9.0	505.2	83.9
				ERZ-EW	9.0	486.6	64.3
Northridge, USA	1994	DWP 77 Rinaldi Receiving Station	6.7	RRS228	10.9	822.1	166.1
				RRS318	10.9	463.0	73.0
Hanshin (Kobe), Japan	1995	CUE 99999 Shin-Osaka	6.9	SHI000	46.0	238.4	37.8
				SHI090	46.0	208.0	27.9
		JMA 99999 KJMA	6.9	KJM000	18.3	805.4	81.3
				KJM090	18.3	587.6	74.3
Duzce, Turkey	1999	ERD 99999 Bolu	7.1	BOL000	41.3	714.2	56.4
				BOL090	41.3	806.4	62.1
		ERD 99999 Duzce		DZC180	1.6	341.4	60.0
				DZC270	1.6	524.8	83.5
Lefkas, Greece	2003	Lefkas 1	6.2	LEF065	12.0	333.4	14.7
				LEF335	12.0	408.6	15.7

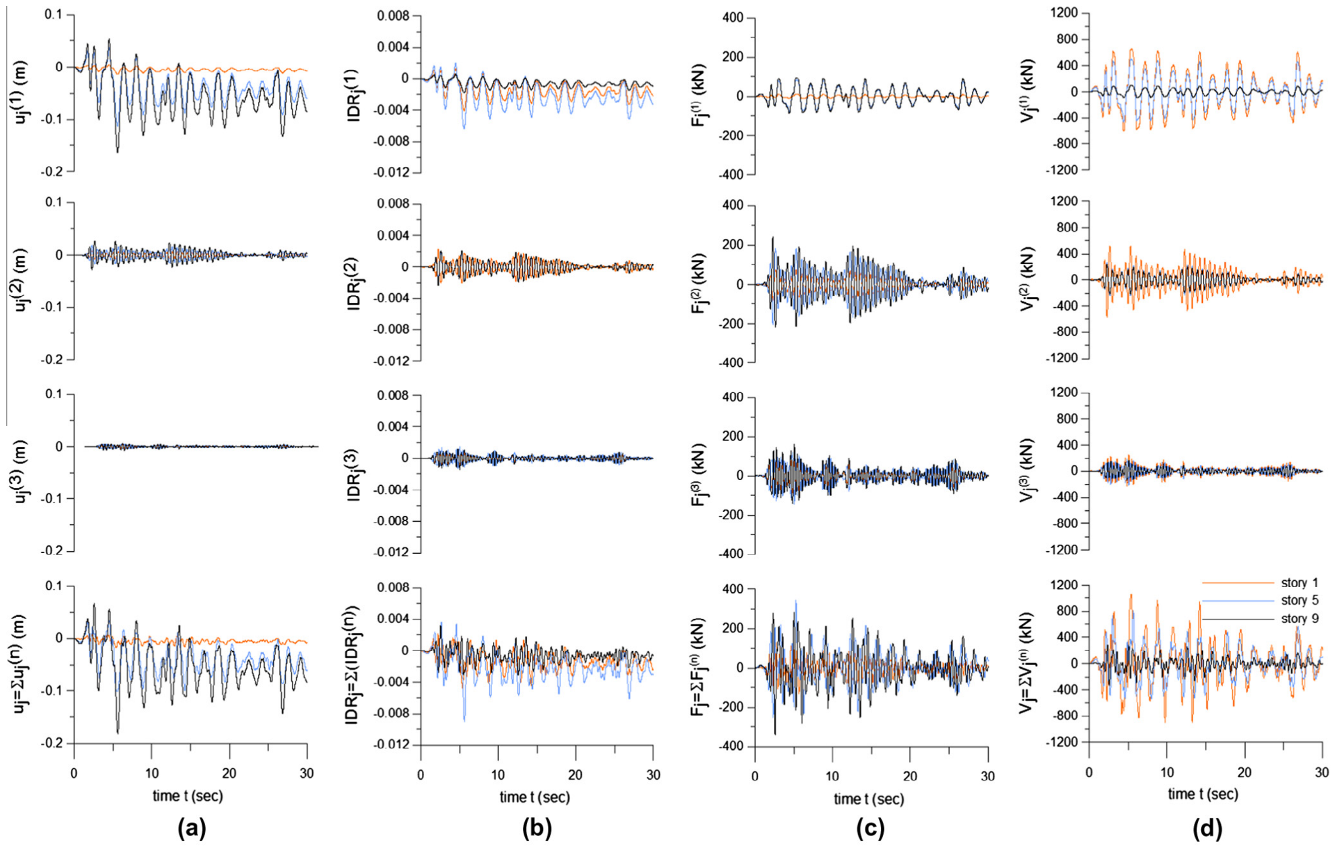

Fig. 4. Time histories of the response at selective storey levels for the 1st mode (top line), the 2nd mode (second line), the 3rd mode (third line) and totally (bottom line), obtained using UMRHA: (a) displacements; (b) inter-storey drifts; (c) storey inertial forces; (d) storey shear forces (ELC180 component of Imperial Valley, 1940, earthquake).

ground excitation, only the first mode response is inelastic, with reduction factor R_{y1} = 2.53 and ductility μ_1 = 2.58, while the second and the third modes respond elastically. Since $R_{y1} \cong \mu_1$, the equal displacement rule is valid and the inelastic response of the first mode can be estimated from the elastic displacement response spectrum. The first eigenperiod (T_1 = 1.68 s) corresponds to the ascending branch of the displacement spectrum and, thus, the first mode comprises a greater value of spectral displacement, *SD*, than the 2nd or the 3rd modes which have periods T_2 = 0.66 s and T_3 = 0.40 s, respectively (Table 1). These lower values of spectral displacement for the higher modes are further reduced concerning the displacement at each level, as they are multiplied by the corresponding participation factors Γ_n < 1.0 (Table 1).

The contribution of higher modes to the response, however, is significant when the inter-storey drifts (*IDR*s) are considered, as shown in Figs. 4b and 5b. In this case, the second mode contributes to the response of the upper floors as much as the first one. The more significant effects of the higher modes on *IDR* than on storey displacements is attributed to the fact that *IDR* is affected by the relative displacements of adjacent storeys, i.e. by φ_{jn}–$\varphi_{j-1,n}$, which are generally larger for the higher modes at the upper storeys. Thus, the first mode is characterized by smoother φ_{jn}–$\varphi_{j-1,n}$ distributions and larger D_n and Γ_n values, whereas the second mode is characterized by larger φ_{jn}–$\varphi_{j-1,n}$ changes and smaller D_n and Γ_n values. The "competition" between these parameters determines the extent of the contribution of the higher modes to *IDR*.

Concerning the inertial forces F_j that develop at the floors, the contribution of higher modes is very important along the whole height of the frame and can be larger than the contribution of the first mode, as shown in Figs. 4c and 5c. It must be noted, however, that the contribution of the 2nd and the 3rd modes on the floor accelerations is somehow exaggerated for the specific base excitation, because they responded elastically, while the 1st mode yielded. It must also be noticed that typically, the spectral accelerations of the higher modes are larger than the one of the first mode, since the first period is usually located outside the acceleration-sensitive area of the response spectrum, which counter counts their smaller participation factors Γ_n. For the El Centro earthquake under consideration, the inertial forces of the 1st mode at the top floor were smaller than the ones of both the 2nd and the 3rd modes (Fig. 4c). Similar observations were made for nearly all the seismic events examined.

The contribution of higher modes is also important for the estimation of storey shear forces, as shown in Figs. 4d and 5d. Although the first mode dominates, the 2nd and the 3rd modes contribute to the total shear with a significant high-frequency component, which increases considerably the maximum values.

4.2. Evaluation of the methods of analysis

In order to assess the accuracy of the methods of analysis presented in Section 2, the response of the RC planar frame was calculated for all 34 ground motions shown in Table 2. The results of the NLRHA were serving as the basis of comparison in order to assess the accuracy of the other methods.

The envelopes of the maximum storey displacements, inter-storey drifts, storey inertial forces and storey shear forces, obtained with the above-mentioned methods, plus a modified version of the mMRSA, denoted as nmMRSA, are depicted in Fig. 7 for the ELC180 component of the Imperial Valley (1940) earthquake. Method nmMRSA is similar to mMRSA with the exception that it assumes inelastic response only for mode 1 and elastic response for the rest modes.

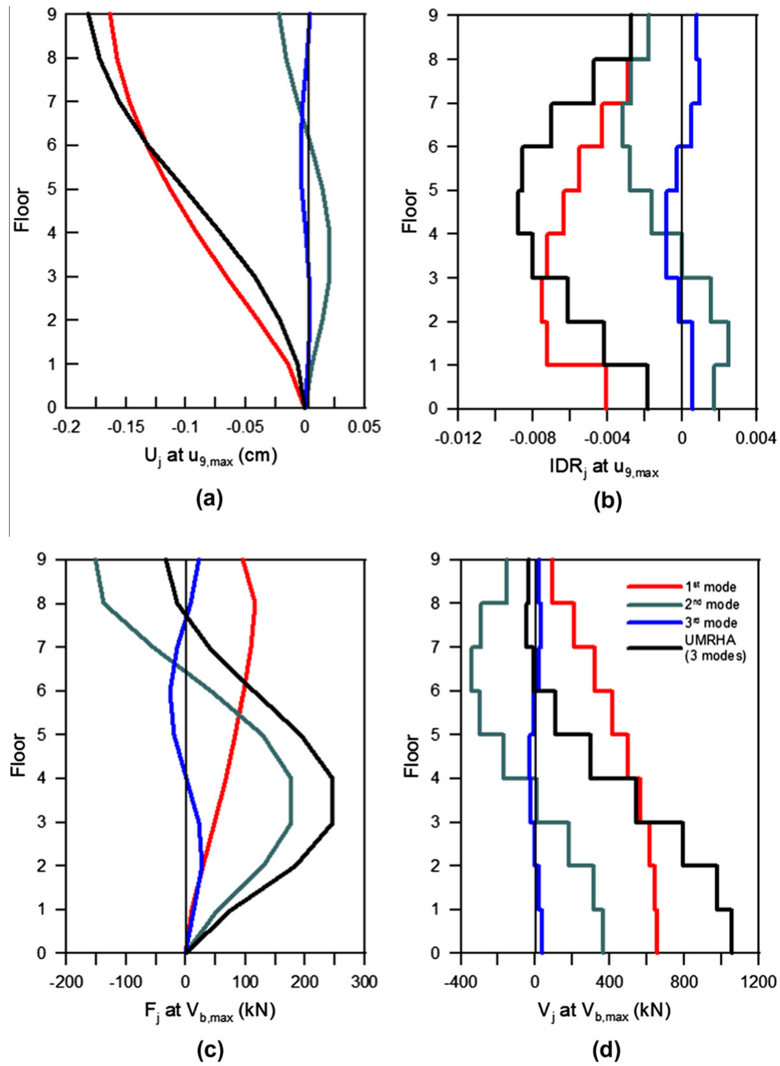

Fig. 5. Snapshots of (a) floor displacement; (b) storey drifts; (c) storey inertial forces; (d) storey shear forces for the ELC180 component of the Imperial Valley (1940) earthquake. Plots (a) and (b) correspond to the time of maximum top displacement and plots (c) and (d) to the time of maximum base shear.

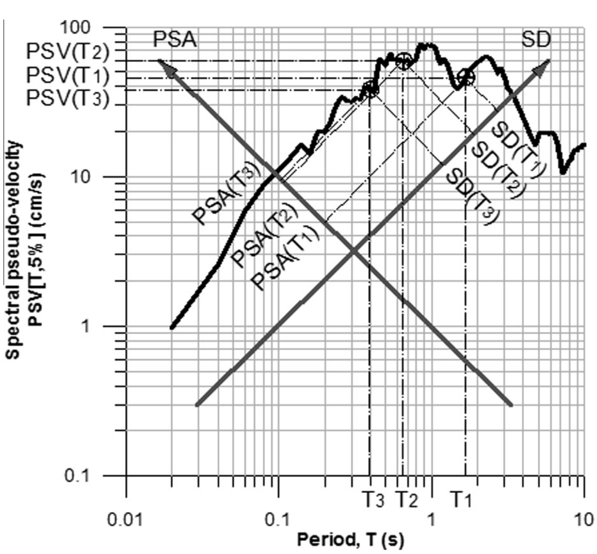

Fig. 6. Response spectrum for component ELC180 of the Imperial Valley (1940) earthquake.

Fig. 7a shows that all methods estimate accurately the storey displacements. The results regarding the inter-storey drifts are similar for all methods (Fig. 7b) with method N2 generally showing the smallest values and UMRHA the largest. Note that N2 is based on first mode only, thus it is reasonable to underestimate the storey drifts at the upper floors, where the contribution of the higher modes is more pronounced.

The distribution of inertial forces shown in Fig. 7c confirms that the role of higher modes in storey accelerations and forces is important. In general, the distribution of the envelope of the lateral forces resembles the uniform distribution. Method N2, by considering only the first mode, significantly underestimates the real response. The extended N2 method presents enhanced accuracy compared to the standard N2 method at the upper floors. It should be mentioned that the calculations regarding the storey inertial and shear forces according to the extended N2 method, even though they refer to global and not local quantities, have been derived using correction factors that correspond to storey drifts, since it was found that the use of these correction factors enhances the accuracy of the method, especially regarding the average storey shears. The rest methods, which consider three modes, produce results close to the ones of NLRHA, with MMPA and mMRSA showing the most accurate results. For all methods, a general trend is

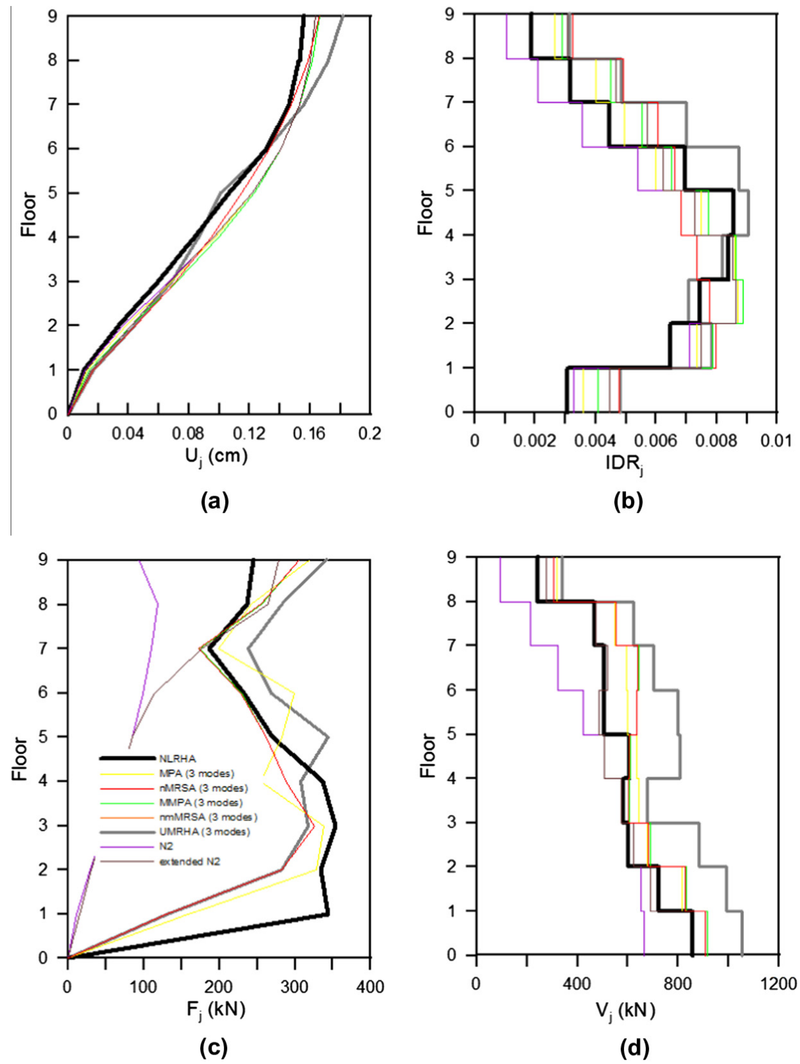

Fig. 7. Envelopes of (a) floor displacement; (b) storey drifts; (c) storey inertial forces; (d) storey shear forces for the ELC180 component of the Imperial Valley (1940) earthquake.

observed: they underestimate the forces at the lower floors and overestimate them at the upper. UMRHA succeeds in estimating satisfactorily the forces at all levels. It is noted that the good accuracy of MMPA shown in Fig. 7 is attributed to the fact that modes 2 and 3 respond elastically to the El Centro ground motion for which the plots were drawn. For other excitations, in which the higher modes respond inelastically, the obtained accuracy was not similarly good.

Concerning shear forces (Fig. 7d), method N2, which considers only the first mode, underestimates the results, especially at the upper storeys, while extended N2, which includes the higher mode contributions, presents acceptable accuracy along height. MPA, MMPA and mMRSA appear to give the closer results to NLRHA. UMRHA slightly overestimates the response at all levels, predicting though correctly the distribution of the shear forces along the height of the frame.

For the entire set of ground motions examined (Table 2), the error of each method of analysis in displacements, inter-storey drifts, storey inertial forces and storey shear forces, determined with respect to the results of NLRHA, was calculated. The results are shown in Fig. 8, where the curves that correspond to the mean value of the error and the mean plus or minus one standard deviation are also plotted. The errors shown in Fig. 8 correspond to the envelope of the response predicted by each method and were calculated by

$$\varepsilon = \frac{|C_{j,Method}| - |C_{j,NLRHA}|}{|C_{j,NLRHA}|} \tag{10}$$

where $C_{j,Method}$ is the maximum response parameter for the jth floor according to each method and $C_{j,NLRHA}$ is the corresponding value obtained by NLRHA. The parameter C can be displacement, inter-storey drift, storey inertial force, or storey shear force. A negative value of ε indicates an unconservative estimation of the response. Note that in Fig. 8, the results of UMRHA for the first mode only and for the first and the second modes are also shown in order to further illustrate the effect of the higher modes.

As depicted in Fig. 8a, the error in displacements is small for all methods, especially at the upper floors; however, although ε is larger at the lower floors, the corresponding displacements are small and the error in absolute terms is smaller than that at the upper floors. MPA and N2 have an average error of less than 10% at all levels, while UMRHA, mMRSA and nmMRSA present competing reliability at the middle storeys. Comparing the results of UMRHA for mode 1 only, modes 1 and 2, and modes 1, 2 and 3 (third column in Fig. 8a), the previously drawn conclusion, that the effect of higher modes on the storey displacements is not important, is verified.

In Fig. 8b, the errors in inter-storey drifts are shown. For all methods, the errors are larger at the upper and lower floors and smaller at mid-height. MPA shows the smallest errors, less than 10% at all levels except the upper floor where the error is less than 20%. UMRHA with 3 modes, nMRSA and nmMRSA give conservative results for the inter-storey drifts at the upper and lower storeys, with errors ranging from 40% to 52%. N2 presents the largest negative values of ε, underestimating the inter-storey drifts especially at the upper floors. Extended N2 presents similar error amplitudes, but overestimates the response, in general. Similar errors with N2 were obtained with UMRHA when only the first mode was used; the addition of the second and third modes did not decrease the amplitude of the error, but produced positive values of ε, yielding results to the safety side.

Concerning the floor inertial forces and the storey shear forces (Fig. 8c and d), nMRSA seems to be the more accurate, with errors less than 23% at all levels. The worst results were obtained with N2 and UMRHA for the 1st mode only, showing errors from −30% to −95% for the inertial forces and from 15% to −70% for the storey shears, which were in the unsafe side in most cases. Addition of the 2nd and the 3rd mode in UMRHA significantly reduced the error. The other methods present similar accuracy, with errors ranging from about −50% for the inertial forces and from −25% for the storey shears to more than 100% for both cases. It is interesting to note that the extended N2 significantly improves the results compared to the standard N2 method specially as regards the storey shears at all levels and inertial forces at higher storeys.

As evident from Fig. 8, the mean error significantly varies along height, even for the same method, depending on the response quantity examined. For this reason, it would be difficult to define a unified error parameter to represent the accuracy of each method. In Fig. 9, the average value of the mean error along height is depicted. It is shown that the average error along height is strongly related to the response parameter examined; thus, smaller values of error are related to storey displacements and inter-storey drifts, while more significant errors are observed in the estimation of storey shears and inertial forces. Methods that consider only the first mode of vibration, such as the N2 method and the UMRHA for the first mode only, present the most significant average error along height. The MPA method for three modes, the UMRHA method including more modes beyond the first one and the mMRSA method present more uniform values of average error regardless of the response parameter examined. The MMPA and the nmMRSA methods, that consider elastic response for the higher modes, seem to

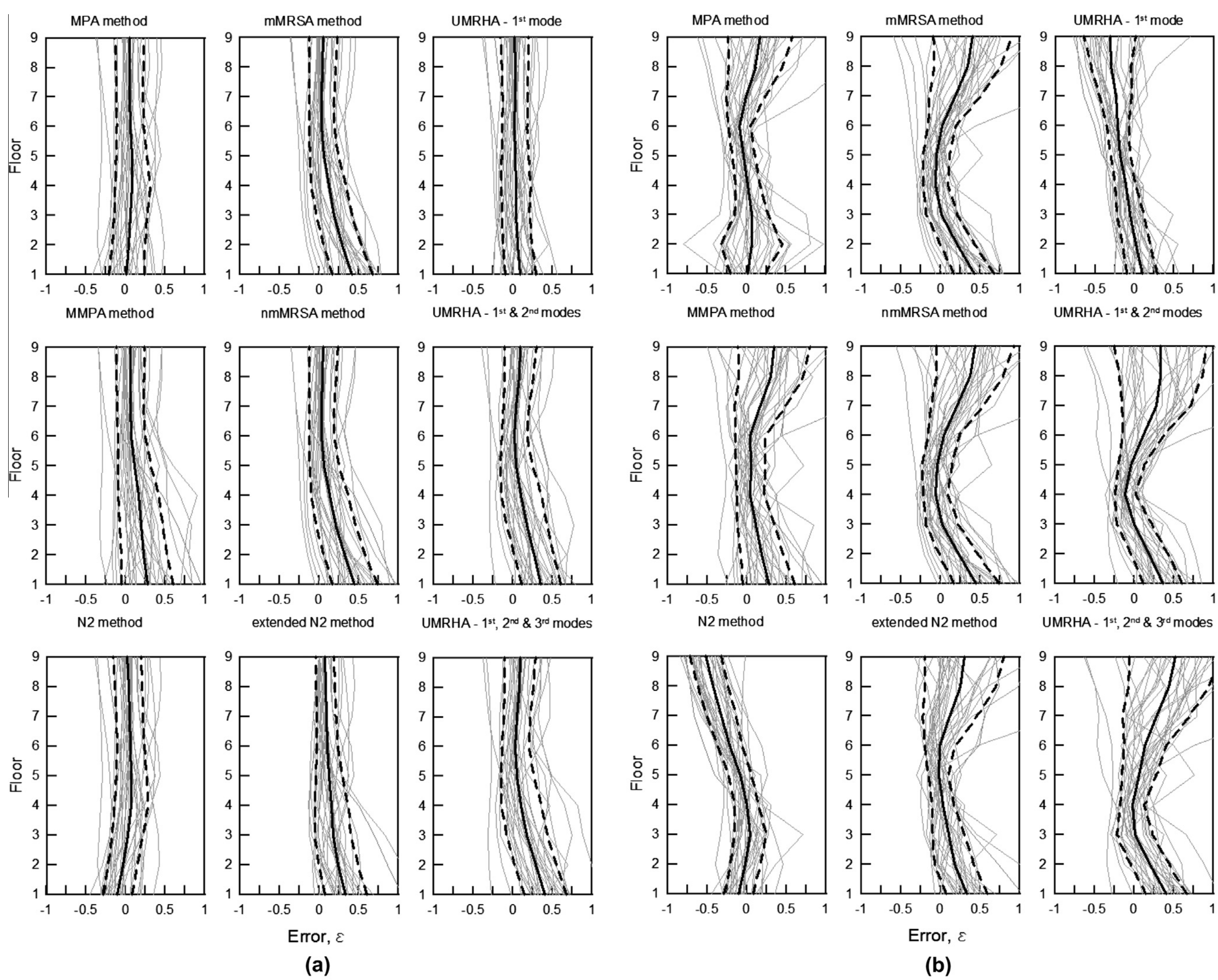

Fig. 8. Errors in (a) floor displacement; (b) storey drifts; (c) storey inertial forces; (d) storey shear forces; of each method examined and for all records considered. Dark solid line shows the mean value and dashed lines the mean plus/minus one standard deviation.

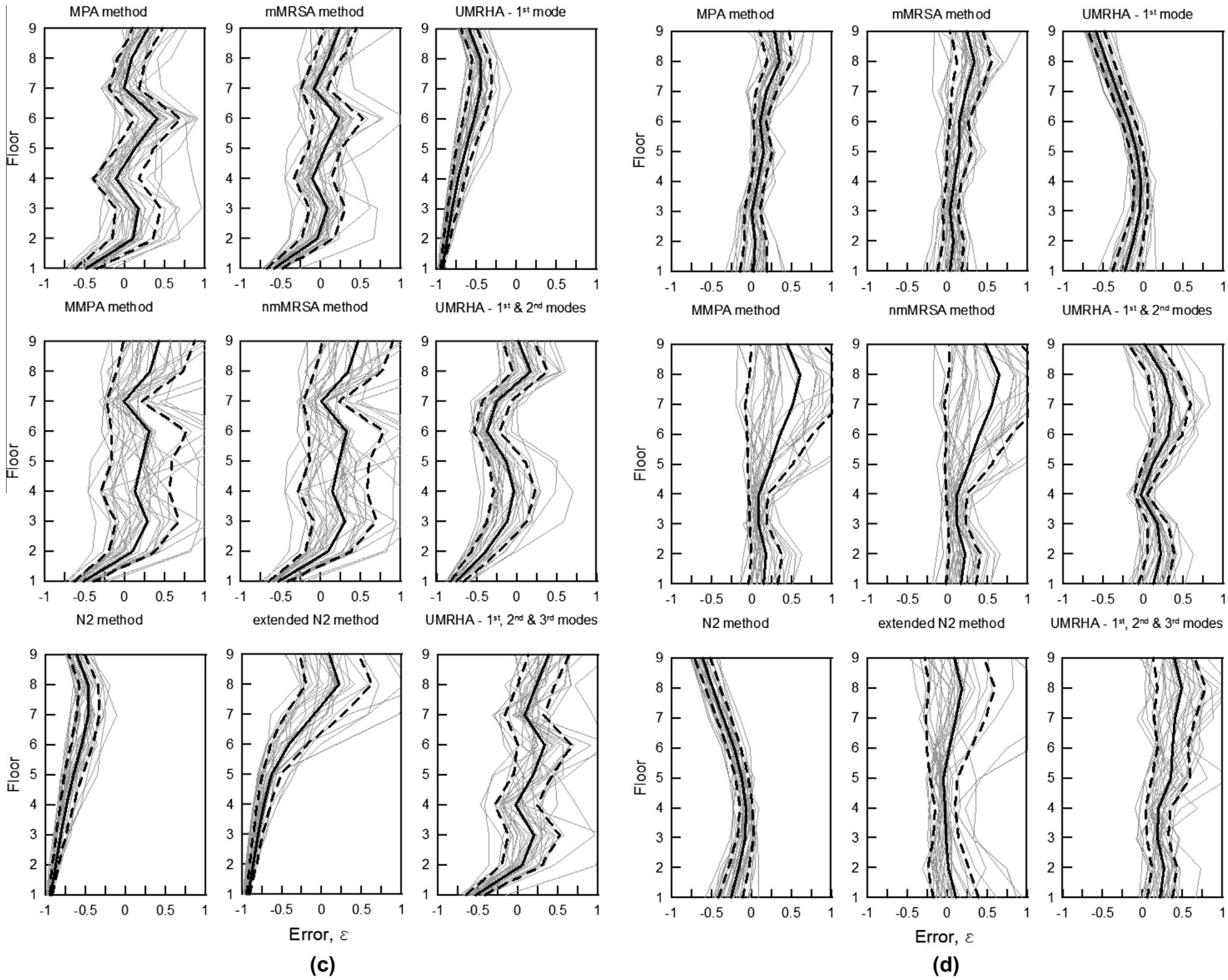

Fig. 8 (*continued*)

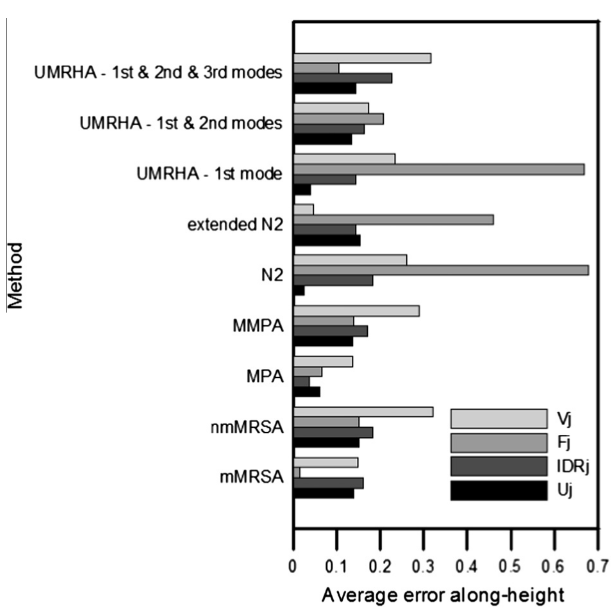

Fig. 9. Average error along height.

introduce more significant errors when the storey shears are examined.

5. Design applications

The above-presented results show that higher modes are important for the seismic design of structures, especially concerning storey forces and shears. Up to now, higher mode effects have been focused on the nonlinear response of MDOF structures with a lateral resisting system consisting of shear walls. However, many recent experimental and analytical results and several failures observed during recent earthquakes enforce the opinion that higher modes are responsible for unexpectedly high values of storey accelerations and shears also in frame structures.

According to current design practice, higher modes are considered through the standard MRSA, using a unique value for the reduction factor R for all modes. This approach, however, underestimates the contribution of the higher modes to the floor accelerations. In a more accurate analysis, different reduction factor R_{yn} for each mode should be used, which would require pushover analyses for all significant modes.

It is noticed that floor accelerations and related inertial forces are important in several structures, as for example in precast buildings in which the forces that develop in the beam–column

Table 3
Behaviour (reduction) and ductility factors for the equivalent inelastic SDOF systems.

No.	Record[a]	Behaviour (reduction) factor			Ductility factor		
		R_{y1}	R_{y2}	R_{y3}	μ_1	μ_2	μ_3
1	BUI000	1.47	0.52	0.09	1.22	0.52	0.09
2	BUI270	0.62	0.36	0.14	0.62	0.36	0.14
3	KAL-L	2.31	0.94	0.40	1.58	0.94	0.40
4	KAL-T	1.97	1.01	0.51	1.69	1.01	0.51
5	LEF065	2.85	1.68	0.61	2.25	1.26	0.61
6	LEF335	2.06	1.98	0.84	1.93	1.52	0.84
7	CXO225	1.26	0.60	0.43	1.23	0.60	0.43
8	CXO315	2.06	0.42	0.19	1.53	0.42	0.19
9	HVP225	2.08	0.74	0.33	2.68	0.74	0.33
10	HVP315	3.19	0.52	0.34	3.63	0.52	0.34
11	E05140	3.70	0.83	0.55	7.09	0.83	0.55
12	E05230	4.35	0.97	0.81	Collapse		
13	TMZ000	1.42	0.49	0.44	1.43	0.49	0.44
14	TMZ270	1.08	1.67	0.52	1.08	1.37	0.52
15	PCD164	9.73	1.09	1.75	9.43	1.09	1.45
16	PCD254	4.40	1.76	1.47	3.29	1.92	1.37
17	ERZ-NS	9.68	1.23	0.48	Collapse		
18	ERZ-EW	4.78	1.83	0.47	4.95	1.79	0.47
19	RRS228	9.73	1.09	1.75	Collapse		
20	RRS318	6.63	1.56	0.85	5.93	1.59	0.85
21	G03000	1.82	1.00	0.66	1.75	1.00	0.66
22	G03090	4.79	0.64	0.29	3.18	0.64	0.29
23	SHI000	1.72	1.48	0.32	2.18	1.44	0.32
24	SHI090	3.06	1.12	0.34	1.63	1.13	0.34
25	KJM000	8.28	3.28	1.38	5.29	3.87	1.28
26	KJM090	4.97	3.15	1.38	6.19	3.14	1.37
27	ELC180	2.53	0.95	0.37	2.58	0.95	0.37
28	ELC270	2.42	0.71	0.35	2.30	0.71	0.35
29	BOL000	4.01	1.51	0.98	3.53	1.46	0.96
30	BOL090	3.42	1.97	0.84	2.80	1.66	0.84
31	DZC180	4.24	1.43	1.10	4.49	1.43	1.08
32	DZC270	6.04	1.81	0.62	6.39	1.94	0.62
33	TAF021	1.37	0.61	0.22	1.41	0.61	0.22
34	TAF111	2.27	0.49	0.24	1.88	0.49	0.24

[a] For corresponding earthquake see Table 2.

connections and floor–beam connections depend on the seismic loads of the floors. It is evident that, if a unique reduction factor for all modes were used in the design of such connections, the resulting joint forces would have been significantly underestimated. Thus, the importance of the correct consideration of the higher modes becomes crucial, even for first-mode dominated structures.

The reduction factors R_{yn} and the displacement ductilities μ_n that were developed for all examined records are collected in Table 3 and graphically depicted in Fig. 10. It is seen that the reduction factors have different values for each mode, which proves the validity of the above statement. In general, there is a trend of R_y to decrease with increasing order of mode, i.e., $R_{y1} \geqslant R_{y2} \geqslant R_{y3}$, as has also been observed by other researchers [23]; however, this observation cannot be generalized, since it is attributed to the flexural overstrength that develops when the frame is deformed according to the second and third modes. As shown in Table 1, the 2nd and the 3rd modes of the structure under consideration yield for significantly higher values of the ratio F_{sny}/L_n than the 1st mode, namely 0.60 g and 1.65 g, respectively. These large yield accelerations of the higher modes would require high spectral accelerations to provoke inelastic modal response. This flexural overstrength of the higher modes, which however might not be as much pronounced in other structures, results in values of R_{y2} and R_{y3} smaller than R_{y1}, as shown in Fig 10b and c respectively. There are only a few points that lie on the $R_{y2} = R_{y1}$ line, as shown in Fig. 10b, while many points of the R_{y2} - $\sim R_{y1}$ space lie below the R_{y2} = 1.00 line, denoting elastic response according to the second mode. As regards the response of the third mode, elastic behaviour is noted for the majority of the records, as shown in Fig 10a and c. Further research is needed on this subject, as the factors that affect and control the flexural overstrength of higher modes have not been investigated enough.

It is evident from the above discussion that the reduction factor that will be developed in each mode depends on the excitation characteristics. For example, for the PCD164 component of the San Fernando (1971) earthquake and the RRS228 component of the Northridge (1994) earthquake, the elastic spectral acceleration for the 3rd eigenperiod is quite large, resulting to a reduction factor R_{3y} larger than R_{2y}. Similar observations were made by Sasaki et al. [31] who reported cases in which the first mode remained elastic while higher modes responded nonlinearly.

When inelastic analyses are performed, the investigation reported herein showed that all methods examined predict satisfactorily storey displacements and inter-storey drifts. Concerning storey forces and shears, MPA and mMRSA, which consider higher modes in a more accurate way than the other methods, produce the closest to the NLRHA results. N2, which is based on the first mode only, failed to predict accurately the floor accelerations, while the extended N2 seems to underestimate the inertial forces and slightly overestimate the floor shear forces along the entire height, with the error depending on the actual values of R_{yn} that are developed.

6. Conclusions

The assessment of the effect of higher modes on the nonlinear response of a 9-storey RC frame is investigated for 34 strong earthquake records using the Uncoupled Modal Response History

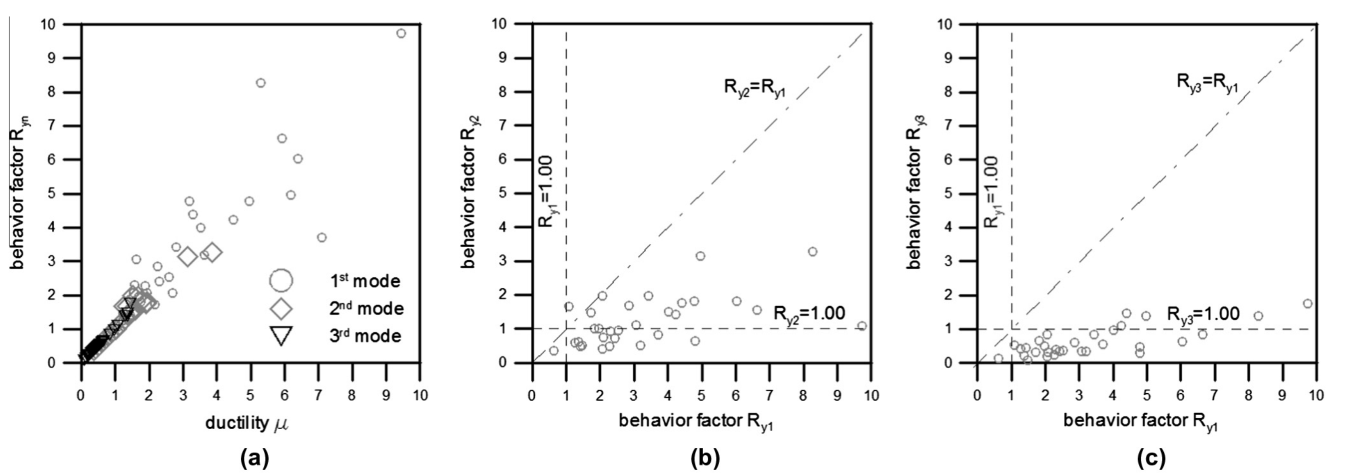

Fig. 10. Behaviour and ductility factors: (a) relationship between the behaviour factor R_{yn} and ductility μ_n; (b) relationship between the behaviour factors R_{y2} and R_{y1}; (c) relationship between the behaviour factors R_{y3} and R_{y1}.

Analysis (UMRHA) method. Additionally, the accuracy obtained by several methods which have been proposed in the literature to estimate the nonlinear response taking under consideration the contribution of higher modes to the response (MPA, MMPA, UMRHA, extended N2, mMRSA) is evaluated by comparing the results with the ones of the Non-Linear Response History Analysis (NLRHA). The comparison is not restricted to storey displacements and inter-storey drifts, but it is extended to floor inertial forces and shears, which are of major importance for the design of several structural types, such as precast buildings with hinged beam–column and floor–beam connections.

Based on the results of this investigation, the following conclusions can be drawn:

(a) Higher mode effects are significant even for planar, first-mode dominated RC frames, especially regarding inertial forces and storey accelerations at all floors and shear forces at higher storeys. Displacements and inter-storey drifts are affected significantly less.
(b) The contribution of higher modes to the storey inertial forces and shear forces depends on the ground motion characteristics and the flexural overstrength associated with each mode.
(c) The modal reduction factors R_{yn} that develop during earthquakes are different for each mode and generally decrease with increasing mode order. The adoption of a unique value of R for all modes, which is determined from the response of the first mode, as is the current design practice, underestimates the storey accelerations and forces significantly. On the other hand, the assumption of linearly elastic response for higher modes might overestimate the response.
(d) The mMRSA method can predict both deformation and force quantities satisfactorily, competing in accuracy with the MPA method. These methods provide the means to estimate the modal reduction factors R_{yn} for a given base excitation, which can be used to design structural and non-structural components.
(e) The MMPA and the extended N2 methods provide acceptable results on the average, except of the underestimation of the inertial forces by extended N2; however, their accuracy depends on the satisfaction of the assumption for elastic higher mode response.
(f) The standard N2 method estimates the displacements satisfactorily but significantly underestimates the storey accelerations and forces.

References

[1] Blakeley RWG, Cooney RC, Megget LM. Seismic shear loading at flexural capacity in cantilever wall structures. Bull NZ Soc Earthq Eng 1975;8:278–90.
[2] Kabeyasawa T, Ogata K. Ultimate-state design of R/C wall-frame structures. Trans Jpn Concr Inst 1985;6:629–36.
[3] Keintzel E. Ductility requirements for shear wall structures in seismic areas. In: Proc of the 8th world conference on earthquake engineering, vol. 5; 1984. p. 671–7.
[4] Paulay T, Priestley MJN. Seismic design of reinforced concrete and masonry buildings. New York: John Wiley & Sons; 1992.
[5] Chopra A. Dynamics of structures: theory and applications to earthquake engineering. 3rd ed. Upper Saddle River: Pearson Prentice Hall; 2007.
[6] Rutenberg A, Nsieri E. The seismic shear demand in ductile cantilever wall systems and the EC8 provisions. Bull Earthq Eng 2006;4:1–21.
[7] Pennucci D, Sullivan TJ, Calvi GM. Evaluation of higher mode effects in tall building response. In: Proc of the 14th European conference on earthquake engineering, vol. 8; 2010. p. 5879–86.
[8] Rejec K, Isaković T, Fischinger M. Seismic shear force magnification in RC cantilever structural walls, designed according to Eurocode 8. Bull Earthq Eng 2012;10:567–86.
[9] Rutenberg A. Seismic shear demand on RC structural walls: review and bibliography. In: Proc of the 3rd international conference on computational methods in structural dynamics and earthquake engineering COMPDYN, paper no 330; 2011.
[10] Earthquake Engineering Research Institute. Northridge earthquake January 17, 1994, preliminary reconnaissance report. In: Hall JF, technical editor. Earthquake spectra, supplement C to vol. 11, publication 95-03. El Cerrito, CA: EERI; 1995.
[11] Earthquake Engineering Research Institute. In: Wyllie Jr LA, Filson JR, editors. Armenia earthquake reconnaissance report. Earthquake spectra publication 89-01. Special supplement. EERI; 1989.
[12] Restrepo JI, Cowan H. The "EJE Cafetero" earthquake, Colombia of January 25, 1999. Bull NZ Soc Earthq Eng 2000;33(1):1–29.
[13] Villaverde R. Explanation for the numerous upper floor collapses during the 1985 Mexico City earthquake. Earthq Eng Struct Dynam 1991;20:223–41.
[14] Wood S, Stanton J, Hawkins N. New seismic design provisions for diaphragms in precast concrete parking structures. PCI J 2000;45(1):50–65.
[15] Rodriguez ME, Blandon JJ. Analysis of diaphragm forces in a five-story miniature steel building during shaking table tests. In: Proc of the 13th world conference on earthquake engineering, paper no 2132; 2004.
[16] Restrepo J, Naito CJ, Fleischman RB. Development of a seismic design methodology for precast concrete floor diaphragms. In: Walraven JC, Stoelhorst D, editors. Tailor made concrete structures: new solutions for our society. London, UK: CRC Press/Balkema; 2008 [chapter 28].
[17] Hoehler MS, Panagiotou M, Restrepo JI, Silva JF, Floriani L, Bourgund U, et al. Performance of suspended pipes and their anchorages during shake table testing of a seven-story building. Earthq Spectra 2009;25:71–91.
[18] Al Abadi HA, Lam NTK, Gad EF, Chandler AM. Earthquake floor spectra for unrestrained building components. Int J Struct Stab Dynam 2004;4(3):361–77.
[19] Shooshtari M, Saatcioglu M, Naumoski N, Foo S. Floor response spectra for seismic design of operational and functional components of concrete buildings in Canada. Can J Civil Eng 2010;37(12):1590–9.
[20] Kumar R, Singh Y, Tripathi S. Effect of building performance on floor response spectra. J Struct Eng (Madras) 2011;37(6):422–6.
[21] Chao SH, Goel SC, Lee SS. A seismic design lateral force distribution based on inelastic state of structures. Earthq Spectra 2007;23(3):547–69.
[22] Panagiotou M, Restrepo JI, Conte JP. Shake table test of a 7-story full scale reinforced concrete wall building slice. Phase I: rectangular wall. ASCE J Struct Eng 2011;137(6):691–705.
[23] Rodriguez ME, Restrepo JI, Carr AJ. Earthquake-induced floor horizontal accelerations in buildings. Earthq Eng Struct Dynam 2002;31:693–718.
[24] Medina RA, Sankaranarayanan R, Kingston KM. Floor response spectra for light components mounted on regular moment-resisting frame structures. Eng Struct 2006;28:1927–40.
[25] Lee HJ, Kuchma D, Aschheim MA. Strength-based design of flexible diaphragms in low-rise structures subjected to earthquake loading. Eng Struct 2007;29(7):1277–95.
[26] Priestley MJN, Sritharan S, Conley J, Pampanin S. Preliminary results and conclusions from the PRESSS five-storey precast concrete test building. PCI J 1999;44(6):42–67.
[27] SAFECAST. Performance of innovative mechanical connections in precast building structures under seismic conditions. Deliverables 5.2. Generalization of results to different structures. FP7 project no 218417; 2012.
[28] Comité Européen de Normalisation CEN. Eurocode 8 – design of structures for earthquake resistance. Part-1. General rules, seismic actions and rules for buildings. Brussels: European Committee for Standardization; 2004.
[29] Priestley MJN, Amaris AD. Dynamic amplification of seismic moments and shears in cantilever walls. Research report no ROSE-2002/01. Pavia: European School for Advanced Studies in Reduction of Seismic Risk; 2002.
[30] Calugaru V, Panagiotou M. Response of tall cantilever wall buildings to strong pulse type seismic excitation. Earthq Eng Struct Dynam 2012;41:1301–18.
[31] Sasaki F, Freeman S, Paret T. Multi-mode pushover procedure (MMP)—a method to identify the effect of higher modes in a pushover analysis. In: Proc of the 6th US national conference on earthquake engineering; 1998.
[32] Paret TF, Sasaki KK, Eilbeck DH, Freeman SA. Approximate inelastic procedures to identify failure mechanisms from higher mode effects. In: Proc of the 11th world conference on earthquake engineering, Acapulco, Mexico, paper 966; 1996.
[33] Priestley MJN. Does capacity design do the job? An examination of higher mode effects in cantilever walls. Bull NZ Soc Earthq Eng 2003;36(4):276–92.
[34] Sullivan TJ, Priestley MJN, Calvi GM. Estimating the higher-mode response of ductile structures. J Earthq Eng 2008;12(3):456–72.
[35] Fajfar P, Fischinger M. N2 – a method for non-linear seismic analysis of regular buildings. In: Proc of the 9th world conference in earthquake engineering, vol. 5; 1988. p. 111–6.
[36] Chopra AK, Goel RK. A modal pushover analysis procedure for estimating seismic demands for buildings. Earthq Eng Struct Dynam 2002;31(3):561–82.
[37] Chopra AK, Goel RK, Chintanapakdee C. Evaluation of a modified MPA procedure assuming higher modes as elastic to estimate seismic demands. Earthq Spectra 2004;20(3):757–78.
[38] Hernández-Montes E, Kwon OS, Aschheim M. An energy-based formulation for first and multiple-mode nonlinear static (pushover) analyses. J Earthq Eng 2004;8(1):69–88.
[39] Kreslin M, Fajfar P. The extended N2 method considering higher mode effects in both plan and elevation. Bull Earthq Eng 2012;10(2):695–715.

[40] Sucuoğlu H, Günay MS. Generalized force vectors for multi-mode pushover analysis. Earthq Eng Struct Dynam 2011;40:55–74.
[41] Kalkan E, Kunnath SK. Adaptive modal combination procedure for nonlinear static analysis of building structures. J Struct Eng (ASCE) 2006;132(1):1721–31.
[42] Antoniou S, Pinho R. Displacement-based adaptive pushover. In Proc of the 2nd international conference on computational methods in structural dynamics and earthquake engineering, COMPDYN, paper no 448; 2009.
[43] Vamvatsikos D, Cornell CA. Incremental dynamic analysis. Earthq Eng Struct Dynam 2002;31:491–514.
[44] American Society of Civil Engineers (ASCE). Minimum design loads for buildings and other structures. ASCE/SEI 7-05. Reston, VA; 2005.
[45] Pacific Earthquake Engineering Research Center (PEER). Tall buildings initiative, guidelines for performance-based seismic design of tall buildings, report 2010/05. Berkeley: PEER; 2010.
[46] Baker JW, Cornell CA. A vector-valued ground motion intensity measure consisting of spectral acceleration and epsilon. Earthq Eng Struct Dynam 2005;34(10):1193–217.
[47] Goel RK, Chopra AK. Evaluation of modal and FEMA pushover analyses: SAC buildings. Earthq Spectra 2004;20(1):225–54.
[48] Dokainish MA, Subbaraj K. A survey of direct time-integration methods in computational structural dynamics – I. Explicit methods. Comput Struct 1989;32(6):1371–86.
[49] Subbaraj K, Dokainish MA. A survey of direct time-integration methods in computational structural dynamics – II. Implicit methods. Comput Struct 1989;32(6):1387–401.
[50] Golley BW. A time-stepping procedure for structural dynamics using gauss point collocation. Int J Numer Meth Eng 1996;39(23):3985–98.
[51] Computers and Structures (CSI), Inc. CSI analysis reference manual for SAP2000, ETABS, and SAFE. Berkeley, CA: Computers and Structures Inc.; 2010.
[52] Chopra AK, Chintanapakdee C. Inelastic deformation ratios for design and evaluation of structures: single-degree-of-freedom bilinear systems. J Struct Eng 2004;130(9):1309–19.
[53] Goel RK, Chopra AK. Role of higher-"mode" pushover analyses in seismic analysis of buildings. Earthq Spectra 2005;21(4):1027–41.
[54] Goel RK, Chopra AK. Extension of modal pushover analysis to compute member forces. Earthq Spectra 2005;21(1):125–39.
[55] Earthquake Planning and Protection Organization (EPPO). Greek aseismic code EAK2000. Athens: EPPO; 2000.
[56] Comité Européen de Normalisation CEN. Eurocode 8 – design of structures for earthquake resistance. Part-3. Assessment and retrofit of buildings. Brussels: European Committee for Standardization; 2005.
[57] PEER strong motion database. <http://www.peer.berkeley.edu>.
[58] Theodulidis N, Kalogeras I, Papazachos C, Karastathis V, Margaris V, Papaioannou Ch, et al. HEAD v. 10: a unified Hellenic accelerogram database. Seismol Res Lett 2004;75(1):36–45.